International Journal of Wildland Fire **2013**, *22*, 970-979
doi:10.1071/WF12028_AC

Supplementary material

Angular variation of fire rate of spread

Jorge C. S. André[A,D]*, João C. Gonçalves*[A,C]*, Gilberto C. Vaz*[B] *and Domingos X. Viegas*[A]

[A]Department of Mechanical Engineering, Faculty of Sciences and Technology, University of Coimbra, Pólo II, Rua Luís Reis Santos, Pinhal de Marrocos, PT-3030-788 Coimbra, Portugal.

[B]Department of Mechanical Engineering, Polytechnic Institute of Coimbra (ISEC), Rua Pedro Nunes, Quinta da Nora, PT-3030-199 Coimbra, Portugal.

[C]Present address: Department of Food Industries, Polytechnic Institute of Viseu (ESAV), Quinta da Alagoa – Estrada de Nelas, Ranhados, PT-3500-606 Viseu, Portugal.

[D]Corresponding author. Email: jorge.andre@dem.uc.pt

(*a*) (*b*)

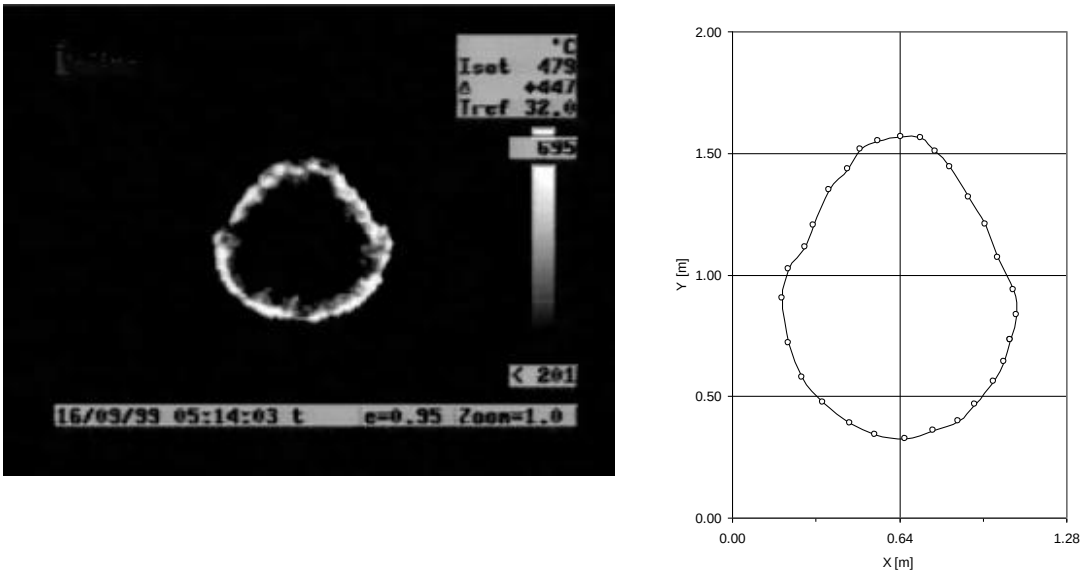

Fig. S1. (*a*) Digitised infrared image obtained in a test with a point ignition in an inclined bed of pine needles. (*b*) Fire line (leading edge of the fire front) captured in the image of Fig. S1*a*, expressed in true physical Cartesian coordinates in the top plane of the fuel bed. The origin O is the bottom left corner of the rectangular fuel bed, the axis OX is the bottom edge of the fuel bed, and the axis OY points up-slope along the left edge of the fuel bed.

(*a*) (*b*)

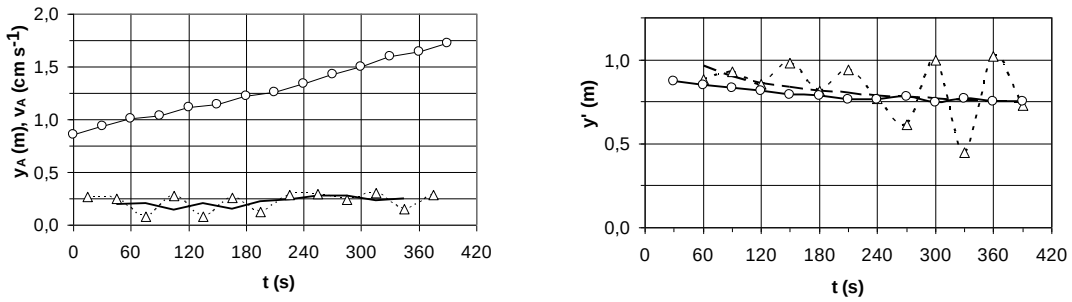

Fig. S2. Application of the first technique to a point ignited fire front of Type II, to determine: (*a*) the coordinate $y_A(t)$ (thin continuous line through open circles) and velocity $v_A(t)$ (thin dashed line through open triangles) of its head A. A moving centred three-point average filter is applied to $v_A(t)$ to capture its trend line (thick continuous line); and (*b***)** the coordinate $y'(t)$ of its (pseudo-) homothetic centre O' with two methods, one that was ultimately abandoned due to its intrinsic numerical instability (dotted line through open triangles and dashed line representing the respective power type trend line) and the adopted one (continuous line through open circles).

(*a*) (*b*)

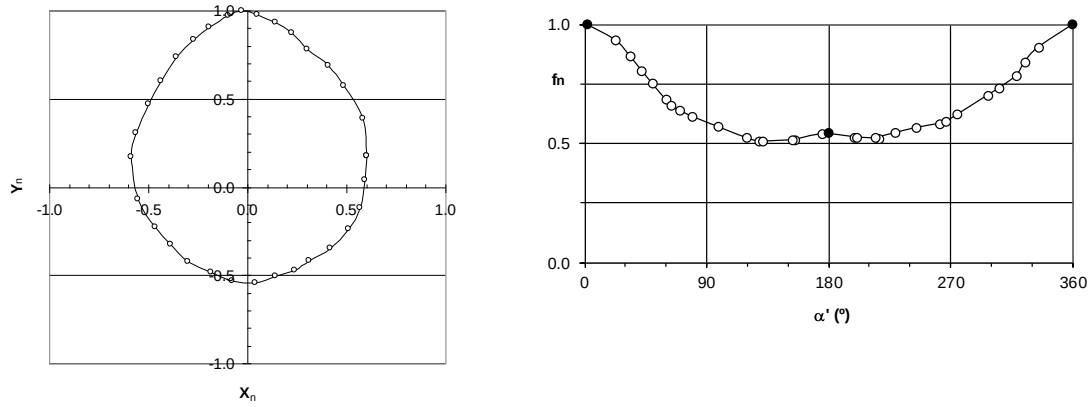

Fig. S3. Analysis of the same fire test of Fig. S2. (*a***)** normalised fire line corresponding to the form function $F(\phi', t = 6{:}30$ min), obtained with the third part of the first technique. (*b***)** orientation function $f_n'(\alpha)$ obtained from the form function of Fig.S3*a* with the second technique, which is enforced to pass through the three points marked with black circles.

(*a*) (*b*)

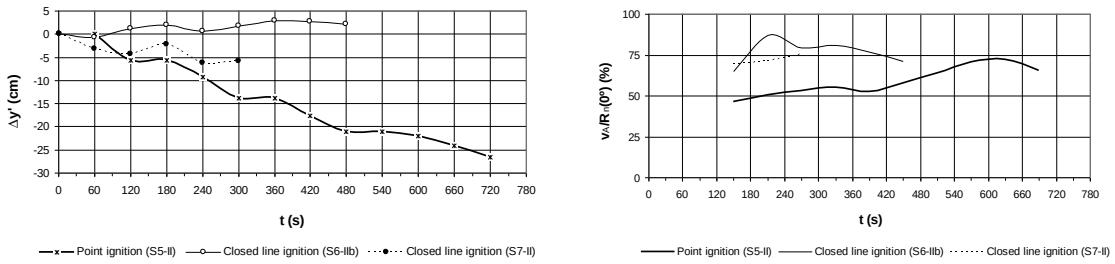

Fig. S4. (*a*) Drift $\Delta y'$ of the homothetic centre O' of the fire line along the longitudinal axis of symmetry of the fuel bed, during tests S5-II, S6-IIb and S7-II. (*b*) Evolution of the non-dimensional velocity $v_A/R_n(0º)$ of the fire front head A, in the same tests. In each case, the rate of spread $R_n(0º)$ is measured in the respective test S#-I.0º. The experimental points (not shown) are fitted with a trend line (three-point moving average filter).

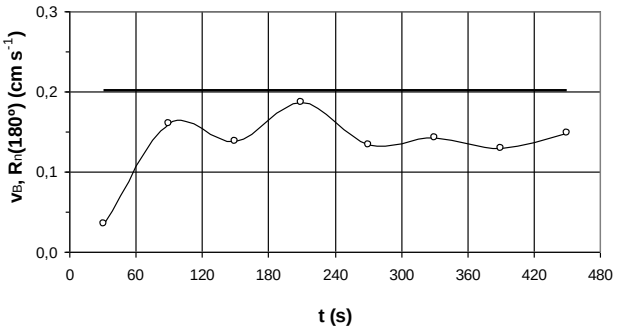

Fig. S5. Evolution of the velocity $v_B(t)$ of the back of the fire line in test S6-IIb (thin line with open symbols) compared with the steady rate of spread of the straight fire front of test S6-I.180º (thick line).